

Evidence for the charmless annihilation decay mode $B_s^0 \rightarrow \pi^+\pi^-$

T. Aaltonen,²¹ B. Álvarez González^{x,9} S. Amerio,⁴⁰ D. Amidei,³² A. Anastassov^{v,15} A. Annovi,¹⁷ J. Antos,¹² G. Apollinari,¹⁵ J.A. Appel,¹⁵ T. Arisawa,⁵⁴ A. Artikov,¹³ J. Asaadi,⁴⁹ W. Ashmanskas,¹⁵ B. Auerbach,⁵⁷ A. Aurisano,⁴⁹ F. Azfar,³⁹ W. Badgett,¹⁵ T. Bae,²⁵ A. Barbaro-Galtieri,²⁶ V.E. Barnes,⁴⁴ B.A. Barnett,²³ P. Barria^{ff,42} P. Bartos,¹² M. Bauced^{dd,40} F. Bedeschi,⁴² S. Behari,²³ G. Bellettini^{ee,42} J. Bellinger,⁵⁶ D. Benjamin,¹⁴ A. Beretvas,¹⁵ A. Bhatti,⁴⁶ D. Bisello^{dd,40} I. Bizjak,²⁸ K.R. Bland,⁵ B. Blumenfeld,²³ A. Bocci,¹⁴ A. Bodek,⁴⁵ D. Bortoletto,⁴⁴ J. Boudreau,⁴³ A. Boveia,¹¹ L. Brigliadori^{cc,6} C. Bromberg,³³ E. Brucken,²¹ J. Budagov,¹³ H.S. Budd,⁴⁵ K. Burkett,¹⁵ G. Busetto^{dd,40} P. Bussey,¹⁹ A. Buzatu,³¹ A. Calamba,¹⁰ C. Calancha,²⁹ S. Camarda,⁴ M. Campanelli,²⁸ M. Campbell,³² F. Canelli^{11,15} B. Carls,²² D. Carlsmith,⁵⁶ R. Carosi,⁴² S. Carrillo^{l,16} S. Carron,¹⁵ B. Casal^{j,9} M. Casarsa,⁵⁰ A. Castro^{cc,6} P. Catastini,²⁰ D. Cauz,⁵⁰ V. Cavaliere,²² M. Cavalli-Sforza,⁴ A. Cerri^{e,26} L. Cerrito^{q,28} Y.C. Chen,¹ M. Chertok,⁷ G. Chiarelli,⁴² G. Chlachidze,¹⁵ F. Chlebana,¹⁵ K. Cho,²⁵ D. Chokheli,¹³ W.H. Chung,⁵⁶ Y.S. Chung,⁴⁵ M.A. Ciocci^{ff,42} A. Clark,¹⁸ C. Clarke,⁵⁵ G. Compostella^{dd,40} M.E. Convery,¹⁵ J. Conway,⁷ M. Corbo,¹⁵ M. Cordelli,¹⁷ C.A. Cox,⁷ D.J. Cox,⁷ F. Crescioli^{ee,42} J. Cuevas^{x,9} R. Culbertson,¹⁵ D. Dagenhart,¹⁵ N. d'Ascenzo^{u,15} M. Datta,¹⁵ P. de Barbaro,⁴⁵ M. Dell'Orso^{ee,42} L. Demortier,⁴⁶ M. Deninno,⁶ F. Devoto,²¹ M. d'Errico^{dd,40} A. Di Canto^{ee,42} B. Di Ruzza,¹⁵ J.R. Dittmann,⁵ M. D'Onofrio,²⁷ S. Donati^{ee,42} P. Dong,¹⁵ M. Dorigo,⁵⁰ T. Dorigo,⁴⁰ K. Ebina,⁵⁴ A. Elagin,⁴⁹ A. Eppig,³² R. Erbacher,⁷ S. Errede,²² N. Ershaidat^{bb,15} R. Eusebi,⁴⁹ S. Farrington,³⁹ M. Feindt,²⁴ J.P. Fernandez,²⁹ R. Field,¹⁶ G. Flanagan^{s,15} R. Forrest,⁷ M.J. Frank,⁵ M. Franklin,²⁰ J.C. Freeman,¹⁵ Y. Funakoshi,⁵⁴ I. Furic,¹⁶ M. Gallinaro,⁴⁶ J.E. Garcia,¹⁸ A.F. Garfinkel,⁴⁴ P. Garosi^{ff,42} H. Gerberich,²² E. Gerchtein,¹⁵ V. Giakoumopoulou,³ P. Giannetti,⁴² K. Gibson,⁴³ C.M. Ginsburg,¹⁵ N. Giokaris,³ P. Giromini,¹⁷ G. Giurgiu,²³ V. Glagolev,¹³ D. Glenzinski,¹⁵ M. Gold,³⁵ D. Goldin,⁴⁹ N. Goldschmidt,¹⁶ A. Golossanov,¹⁵ G. Gomez,⁹ G. Gomez-Ceballos,³⁰ M. Goncharov,³⁰ O. González,²⁹ I. Gorelov,³⁵ A.T. Goshaw,¹⁴ K. Goulianos,⁴⁶ S. Grinstein,⁴ C. Grosso-Pilcher,¹¹ R.C. Group^{53,15} J. Guimaraes da Costa,²⁰ S.R. Hahn,¹⁵ E. Halkiadakis,⁴⁸ A. Hamaguchi,³⁸ J.Y. Han,⁴⁵ F. Happacher,¹⁷ K. Hara,⁵¹ D. Hare,⁴⁸ M. Hare,⁵² R.F. Harr,⁵⁵ K. Hatakeyama,⁵ C. Hays,³⁹ M. Heck,²⁴ J. Heinrich,⁴¹ M. Herndon,⁵⁶ S. Hewamanage,⁵ A. Hocker,¹⁵ W. Hopkins^{f,15} D. Horn,²⁴ S. Hou,¹ R.E. Hughes,³⁶ M. Hurwitz,¹¹ U. Husemann,⁵⁷ N. Hussain,³¹ M. Hussein,³³ J. Huston,³³ G. Introzzi,⁴² M. Iori^{hh,47} A. Ivanov^{o,7} E. James,¹⁵ D. Jang,¹⁰ B. Jayatilaka,¹⁴ E.J. Jeon,²⁵ S. Jindariani,¹⁵ M. Jones,⁴⁴ K.K. Joo,²⁵ S.Y. Jun,¹⁰ T.R. Junk,¹⁵ T. Kamon^{25,49} P.E. Karchin,⁵⁵ A. Kashi,⁵ Y. Kato^{n,38} W. Ketchum,¹¹ J. Keung,⁴¹ V. Khotilovich,⁴⁹ B. Kilminster,¹⁵ D.H. Kim,²⁵ H.S. Kim,²⁵ J.E. Kim,²⁵ M.J. Kim,¹⁷ S.B. Kim,²⁵ S.H. Kim,⁵¹ Y.K. Kim,¹¹ Y.J. Kim,²⁵ N. Kimura,⁵⁴ M. Kirby,¹⁵ S. Klimentenko,¹⁶ K. Knoepfel,¹⁵ K. Kondo^{*,54} D.J. Kong,²⁵ J. Konigsberg,¹⁶ A.V. Kotwal,¹⁴ M. Kreps,²⁴ J. Kroll,⁴¹ D. Krop,¹¹ M. Kruse,¹⁴ V. Krutelyov^{c,49} T. Kuhr,²⁴ M. Kurata,⁵¹ S. Kwang,¹¹ A.T. Laasanen,⁴⁴ S. Lami,⁴² S. Lammel,¹⁵ M. Lancaster,²⁸ R.L. Lander,⁷ K. Lannon^{w,36} A. Lath,⁴⁸ G. Latino^{ee,42} T. LeCompte,² E. Lee,⁴⁹ H.S. Lee^{25,11} J.S. Lee,²⁵ S.W. Lee^{z,49} S. Leo^{ee,42} S. Leone,⁴² J.D. Lewis,¹⁵ A. Limosani^{r,14} C.-J. Lin,²⁶ M. Lindgren,¹⁵ E. Lipeles,⁴¹ A. Lister,¹⁸ D.O. Litvintsev,¹⁵ C. Liu,⁴³ H. Liu,⁵³ Q. Liu,⁴⁴ T. Liu,¹⁵ S. Lockwitz,⁵⁷ A. Loginov,⁵⁷ D. Lucchesi^{dd,40} J. Lueck,²⁴ P. Lujan,²⁶ P. Lukens,¹⁵ G. Lungu,⁴⁶ J. Lys,²⁶ R. Lysak,¹² R. Madrak,¹⁵ K. Maeshima,¹⁵ P. Maestro^{ff,42} S. Malik,⁴⁶ G. Manca^{a,27} A. Manousakis-Katsikakis,³ F. Margaroli,⁴⁷ C. Marino,²⁴ M. Martínez,⁴ P. Mastrandrea,⁴⁷ K. Matera,²² M.E. Mattson,⁵⁵ A. Mazzacane,¹⁵ P. Mazzanti,⁶ K.S. McFarland,⁴⁵ P. McIntyre,⁴⁹ R. McNulty^{i,27} A. Mehta,²⁷ P. Mehtala,²¹ C. Mesropian,⁴⁶ T. Miao,¹⁵ D. Mietlicki,³² A. Mitra,¹ H. Miyake,⁵¹ S. Moed,¹⁵ N. Moggi,⁶ M.N. Mondragon^{l,15} C.S. Moon,²⁵ R. Moore,¹⁵ M.J. Morello^{gg,42} J. Morlock,²⁴ P. Movilla Fernandez,¹⁵ A. Mukherjee,¹⁵ Th. Muller,²⁴ P. Murat,¹⁵ M. Mussini^{cc,6} J. Nachtman^{m,15} Y. Nagai,⁵¹ J. Naganoma,⁵⁴ I. Nakano,³⁷ A. Napier,⁵² J. Nett,⁴⁹ C. Neu,⁵³ M.S. Neubauer,²² J. Nielsen^{d,26} L. Nodulman,² S.Y. Noh,²⁵ O. Norniella,²² L. Oakes,³⁹ S.H. Oh,¹⁴ Y.D. Oh,²⁵ I. Oksuzian,⁵³ T. Okusawa,³⁸ R. Orava,²¹ L. Ortolan,⁴ S. Pagan Griso^{dd,40} C. Pagliarone,⁵⁰ E. Palencia^{e,9} V. Papadimitriou,¹⁵ A.A. Paramonov,² J. Patrick,¹⁵ G. Pauletta^{ii,50} M. Paulini,¹⁰ C. Paus,³⁰ D.E. Pellett,⁷ A. Penzo,⁵⁰ T.J. Phillips,¹⁴ G. Piacentino,⁴² E. Pianori,⁴¹ J. Pilot,³⁶ K. Pitts,²² C. Plager,⁸ L. Pondrom,⁵⁶ S. Poprocki^{f,15} K. Potamianos,⁴⁴ F. Prokoshin^{aa,13} A. Pranko,²⁶ F. Ptohos^{g,17} G. Punzi^{ee,42} A. Rahaman,⁴³ V. Ramakrishnan,⁵⁶ N. Ranjan,⁴⁴ I. Redondo,²⁹ P. Renton,³⁹ M. Rescigno,⁴⁷ T. Riddick,²⁸ F. Rimondi^{cc,6} L. Ristori^{42,15} A. Robson,¹⁹ T. Rodrigo,⁹ T. Rodriguez,⁴¹ E. Rogers,²² S. Rolli^{h,52} R. Roser,¹⁵ F. Ruffini^{ff,42} A. Ruiz,⁹ J. Russ,¹⁰ V. Rusu,¹⁵ A. Safonov,⁴⁹ W.K. Sakumoto,⁴⁵ Y. Sakurai,⁵⁴ L. Santi^{ii,50} K. Sato,⁵¹ V. Savelyev^{u,15} A. Savoy-Navarro^{y,15} P. Schlabach,¹⁵ A. Schmidt,²⁴ E.E. Schmidt,¹⁵ T. Schwarz,¹⁵ L. Scodellaro,⁹ A. Scribano^{ff,42} F. Scuri,⁴² S. Seidel,³⁵ Y. Seiya,³⁸ A. Semenov,¹³ F. Sforza^{ff,42} S.Z. Shalhout,⁷

T. Shears,²⁷ P.F. Shepard,⁴³ M. Shimojima^t,⁵¹ M. Shochet,¹¹ I. Shreyber-Tecker,³⁴ A. Simonenko,¹³ P. Sinervo,³¹ K. Sliwa,⁵² J.R. Smith,⁷ F.D. Snider,¹⁵ A. Soha,¹⁵ V. Sorin,⁴ H. Song,⁴³ P. Squillacioti^{ff},⁴² M. Stancari,¹⁵ R. St. Denis,¹⁹ B. Stelzer,³¹ O. Stelzer-Chilton,³¹ D. Stentz^v,¹⁵ J. Strologas,³⁵ G.L. Strycker,³² Y. Sudo,⁵¹ A. Sukhanov,¹⁵ I. Suslov,¹³ K. Takemasa,⁵¹ Y. Takeuchi,⁵¹ J. Tang,¹¹ M. Tecchio,³² P.K. Teng,¹ J. Thom^f,¹⁵ J. Thome,¹⁰ G.A. Thompson,²² E. Thomson,⁴¹ D. Toback,⁴⁹ S. Tokar,¹² K. Tollefson,³³ T. Tomura,⁵¹ D. Tonelli,¹⁵ S. Torre,¹⁷ D. Torretta,¹⁵ P. Totaro,⁴⁰ M. Trovato^{gg},⁴² F. Ukegawa,⁵¹ S. Uozumi,²⁵ A. Varganov,³² F. Vázquez^l,¹⁶ G. Velev,¹⁵ C. Vellidis,¹⁵ M. Vidal,⁴⁴ I. Vila,⁹ R. Vilar,⁹ J. Vizán,⁹ M. Vogel,³⁵ G. Volpi,¹⁷ P. Wagner,⁴¹ R.L. Wagner,¹⁵ T. Wakisaka,³⁸ R. Wallny,⁸ S.M. Wang,¹ A. Warburton,³¹ D. Waters,²⁸ W.C. Wester III,¹⁵ D. Whiteson^b,⁴¹ A.B. Wicklund,² E. Wicklund,¹⁵ S. Wilbur,¹¹ F. Wick,²⁴ H.H. Williams,⁴¹ J.S. Wilson,³⁶ P. Wilson,¹⁵ B.L. Winer,³⁶ P. Wittich^f,¹⁵ S. Wollbers,¹⁵ H. Wolfe,³⁶ T. Wright,³² X. Wu,¹⁸ Z. Wu,⁵ K. Yamamoto,³⁸ D. Yamato,³⁸ T. Yang,¹⁵ U.K. Yang^p,¹¹ Y.C. Yang,²⁵ W.-M. Yao,²⁶ G.P. Yeh,¹⁵ K. Yi^m,¹⁵ J. Yoh,¹⁵ K. Yorita,⁵⁴ T. Yoshida^k,³⁸ G.B. Yu,¹⁴ I. Yu,²⁵ S.S. Yu,¹⁵ J.C. Yun,¹⁵ A. Zanetti,⁵⁰ Y. Zeng,¹⁴ and S. Zucchelli^{cc6}

(CDF Collaboration[†])

¹*Institute of Physics, Academia Sinica, Taipei, Taiwan 11529, Republic of China*

²*Argonne National Laboratory, Argonne, Illinois 60439, USA*

³*University of Athens, 157 71 Athens, Greece*

⁴*Institut de Física d'Altes Energies, ICREA, Universitat Autònoma de Barcelona, E-08193, Bellaterra (Barcelona), Spain*

⁵*Baylor University, Waco, Texas 76798, USA*

⁶*Istituto Nazionale di Fisica Nucleare Bologna, ^{cc}University of Bologna, I-40127 Bologna, Italy*

⁷*University of California, Davis, Davis, California 95616, USA*

⁸*University of California, Los Angeles, Los Angeles, California 90024, USA*

⁹*Instituto de Física de Cantabria, CSIC-University of Cantabria, 39005 Santander, Spain*

¹⁰*Carnegie Mellon University, Pittsburgh, Pennsylvania 15213, USA*

¹¹*Enrico Fermi Institute, University of Chicago, Chicago, Illinois 60637, USA*

¹²*Comenius University, 842 48 Bratislava, Slovakia; Institute of Experimental Physics, 040 01 Kosice, Slovakia*

¹³*Joint Institute for Nuclear Research, RU-141980 Dubna, Russia*

¹⁴*Duke University, Durham, North Carolina 27708, USA*

¹⁵*Fermi National Accelerator Laboratory, Batavia, Illinois 60510, USA*

¹⁶*University of Florida, Gainesville, Florida 32611, USA*

¹⁷*Laboratori Nazionali di Frascati, Istituto Nazionale di Fisica Nucleare, I-00044 Frascati, Italy*

¹⁸*University of Geneva, CH-1211 Geneva 4, Switzerland*

¹⁹*Glasgow University, Glasgow G12 8QQ, United Kingdom*

²⁰*Harvard University, Cambridge, Massachusetts 02138, USA*

²¹*Division of High Energy Physics, Department of Physics,*

University of Helsinki and Helsinki Institute of Physics, FIN-00014, Helsinki, Finland

²²*University of Illinois, Urbana, Illinois 61801, USA*

²³*The Johns Hopkins University, Baltimore, Maryland 21218, USA*

²⁴*Institut für Experimentelle Kernphysik, Karlsruhe Institute of Technology, D-76131 Karlsruhe, Germany*

²⁵*Center for High Energy Physics: Kyungpook National University,*

Daegu 702-701, Korea; Seoul National University, Seoul 151-742,

Korea; Sungkyunkwan University, Suwon 440-746,

Korea; Korea Institute of Science and Technology Information,

Daejeon 305-806, Korea; Chonnam National University, Gwangju 500-757,

Korea; Chonbuk National University, Jeonju 561-756, Korea

²⁶*Ernest Orlando Lawrence Berkeley National Laboratory, Berkeley, California 94720, USA*

²⁷*University of Liverpool, Liverpool L69 7ZE, United Kingdom*

²⁸*University College London, London WC1E 6BT, United Kingdom*

²⁹*Centro de Investigaciones Energeticas Medioambientales y Tecnológicas, E-28040 Madrid, Spain*

³⁰*Massachusetts Institute of Technology, Cambridge, Massachusetts 02139, USA*

³¹*Institute of Particle Physics: McGill University, Montréal, Québec,*

Canada H3A 2T8; Simon Fraser University, Burnaby, British Columbia,

Canada V5A 1S6; University of Toronto, Toronto, Ontario,

Canada M5S 1A7; and TRIUMF, Vancouver, British Columbia, Canada V6T 2A3

³²*University of Michigan, Ann Arbor, Michigan 48109, USA*

³³*Michigan State University, East Lansing, Michigan 48824, USA*

³⁴*Institution for Theoretical and Experimental Physics, ITEP, Moscow 117259, Russia*

³⁵*University of New Mexico, Albuquerque, New Mexico 87131, USA*

³⁶*The Ohio State University, Columbus, Ohio 43210, USA*

³⁷*Okayama University, Okayama 700-8530, Japan*

³⁸*Osaka City University, Osaka 588, Japan*

- ³⁹University of Oxford, Oxford OX1 3RH, United Kingdom
⁴⁰Istituto Nazionale di Fisica Nucleare, Sezione di Padova-Trento, ^{4d}University of Padova, I-35131 Padova, Italy
⁴¹University of Pennsylvania, Philadelphia, Pennsylvania 19104, USA
⁴²Istituto Nazionale di Fisica Nucleare Pisa, ^{4e}University of Pisa,
^{4f}University of Siena and ^{4g}Scuola Normale Superiore, I-56127 Pisa, Italy
⁴³University of Pittsburgh, Pittsburgh, Pennsylvania 15260, USA
⁴⁴Purdue University, West Lafayette, Indiana 47907, USA
⁴⁵University of Rochester, Rochester, New York 14627, USA
⁴⁶The Rockefeller University, New York, New York 10065, USA
⁴⁷Istituto Nazionale di Fisica Nucleare, Sezione di Roma 1,
^{4h}Sapienza Università di Roma, I-00185 Roma, Italy
⁴⁸Rutgers University, Piscataway, New Jersey 08855, USA
⁴⁹Texas A&M University, College Station, Texas 77843, USA
⁵⁰Istituto Nazionale di Fisica Nucleare Trieste/Udine,
I-34100 Trieste, ⁴ⁱUniversity of Udine, I-33100 Udine, Italy
⁵¹University of Tsukuba, Tsukuba, Ibaraki 305, Japan
⁵²Tufts University, Medford, Massachusetts 02155, USA
⁵³University of Virginia, Charlottesville, Virginia 22906, USA
⁵⁴Waseda University, Tokyo 169, Japan
⁵⁵Wayne State University, Detroit, Michigan 48201, USA
⁵⁶University of Wisconsin, Madison, Wisconsin 53706, USA
⁵⁷Yale University, New Haven, Connecticut 06520, USA
- (Dated: October 31, 2011)

We search for annihilation decay modes of neutral b mesons into pairs of charmless charged hadrons with the upgraded Collider Detector at the Fermilab Tevatron. Using a data sample corresponding to 6 fb^{-1} of integrated luminosity, we obtain the first evidence for the $B_s^0 \rightarrow \pi^+\pi^-$ decay, with a significance of 3.7σ , and a measured branching ratio $\mathcal{B}(B_s^0 \rightarrow \pi^+\pi^-) = (0.57 \pm 0.15 \text{ (stat)} \pm 0.10 \text{ (syst)}) \times 10^{-6}$. A search for the $B^0 \rightarrow K^+K^-$ mode in the same sample yields a significance of 2.0σ , and a central value estimate $\mathcal{B}(B^0 \rightarrow K^+K^-) = (0.23 \pm 0.10 \text{ (stat)} \pm 0.10 \text{ (syst)}) \times 10^{-6}$.

PACS numbers: 13.25.Hw 14.40.Nd

Two-body non-leptonic charmless decays of b hadrons are widely-studied processes in flavor physics. Their investigations enable a deeper understanding of strong-

interaction dynamics with the potential to refine the modeling of these processes by effective theories. Some decays receive contributions from higher-order (‘penguin’) transitions, and are therefore sensitive to the possible presence of new physics in internal loops.

The $B_s^0 \rightarrow \pi^+\pi^-$ and $B^0 \rightarrow K^+K^-$ decay modes have a special status, in that all quarks in the final state are different from those in the initial state. This limits the possible diagrams that contribute to these decays to penguin-annihilation (PA) and W -exchange (E) topologies (see Fig. 1). These amplitudes are difficult to predict within the current phenomenological models and are often neglected in calculations. They can carry different CP -violating and CP -conserving phases with respect to leading-order diagrams, so the lack of knowledge of their size introduces uncertainties in predictions for other well-studied decays, such as $B^0 \rightarrow \pi^+\pi^-$ and $B_s^0 \rightarrow K^+K^-$ [1–4].

Estimates of these amplitudes in the QCD factorization (QCDF) approach [5, 6] are affected by significant uncertainties. No predictions are currently available within the soft collinear effective theory (SCET) [7]. Only recent perturbative QCD calculations (pQCD) provide some potentially testable predictions [8, 9].

Up to now, the $B_s^0 \rightarrow \pi^+\pi^-$ and $B^0 \rightarrow K^+K^-$ decay modes have not been observed; the best upper limits at the 90% confidence level are respectively 1.2×10^{-6} [10]

*Deceased

[†]With visitors from ^aIstituto Nazionale di Fisica Nucleare, Sezione di Cagliari, 09042 Monserrato (Cagliari), Italy, ^bUniversity of CA Irvine, Irvine, CA 92697, USA, ^cUniversity of CA Santa Barbara, Santa Barbara, CA 93106, USA, ^dUniversity of CA Santa Cruz, Santa Cruz, CA 95064, USA, ^eCERN, CH-1211 Geneva, Switzerland, ^fCornell University, Ithaca, NY 14853, USA, ^gUniversity of Cyprus, Nicosia CY-1678, Cyprus, ^hOffice of Science, U.S. Department of Energy, Washington, DC 20585, USA, ⁱUniversity College Dublin, Dublin 4, Ireland, ^jETH, 8092 Zurich, Switzerland, ^kUniversity of Fukui, Fukui City, Fukui Prefecture, Japan 910-0017, ^lUniversidad Iberoamericana, Mexico D.F., Mexico, ^mUniversity of Iowa, Iowa City, IA 52242, USA, ⁿKinki University, Higashi-Osaka City, Japan 577-8502, ^oKansas State University, Manhattan, KS 66506, USA, ^pUniversity of Manchester, Manchester M13 9PL, United Kingdom, ^qQueen Mary, University of London, London, E1 4NS, United Kingdom, ^rUniversity of Melbourne, Victoria 3010, Australia, ^sMuons, Inc., Batavia, IL 60510, USA, ^tNagasaki Institute of Applied Science, Nagasaki, Japan, ^uNational Research Nuclear University, Moscow, Russia, ^vNorthwestern University, Evanston, IL 60208, USA, ^wUniversity of Notre Dame, Notre Dame, IN 46556, USA, ^xUniversidad de Oviedo, E-33007 Oviedo, Spain, ^yCNRS-IN2P3, Paris, F-75205 France, ^zTexas Tech University, Lubbock, TX 79609, USA, ^{aa}Universidad Tecnica Federico Santa Maria, 110v Valparaiso, Chile, ^{bb}Yarmouk University, Irbid 211-63, Jordan.

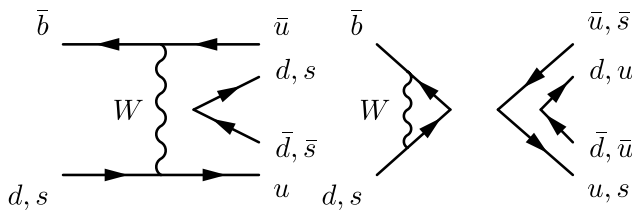


FIG. 1: E (left panel) and PA (right panel) diagrams contributing to $B^0 \rightarrow K^+K^-$ and $B_s^0 \rightarrow \pi^+\pi^-$ decays.

and 0.41×10^{-6} [11]. A measurement of branching fractions of both modes would be particularly useful, since it would allow a better constraint on the strength of PA and E amplitudes [2].

In this Letter we report the results of a simultaneous search for the two decays $B_s^0 \rightarrow \pi^+\pi^-$ and $B^0 \rightarrow K^+K^-$ [12], using data corresponding to 6 fb^{-1} integrated luminosity of $\bar{p}p$ collisions at $\sqrt{s} = 1.96 \text{ TeV}$, collected by the upgraded Collider Detector (CDF II) at the Fermilab Tevatron.

The CDF II detector is described in detail in Ref. [13] with the detector sub-systems relevant for this analysis discussed in Ref. [14]. The data are collected by a three-level on-line event-selection system (trigger). At level 1, tracks are reconstructed in the transverse plane [15]. Two opposite-charge particles are required, with reconstructed transverse momenta $p_{T1}, p_{T2} > 2 \text{ GeV}/c$, the scalar sum $p_{T1} + p_{T2} > 5.5 \text{ GeV}/c$, and an azimuthal opening angle $\Delta\phi < 135^\circ$. At level 2, tracks are combined with silicon-tracking-detector hits and their impact parameter d (transverse distance of closest approach to the beam line) is determined with $45 \mu\text{m}$ resolution (including the beam spread) and required to be $0.1 < d < 1.0 \text{ mm}$. A tighter opening-angle requirement, $20^\circ < \Delta\phi < 135^\circ$, is also applied. Each track pair is then used to form a B candidate, which is required to have an impact parameter $d_B < 140 \mu\text{m}$ and to have travelled a distance $L_T > 200 \mu\text{m}$ in the transverse plane. At level 3, a cluster of computers confirms the selection with a full event reconstruction.

The offline selection is based on a more accurate determination of the same quantities used in the trigger, with the addition of two further observables: the isolation (I_B) of the B candidate [16], and the quality of the three-dimensional fit (χ^2 with one degree of freedom) of the decay vertex of the B candidate. Requiring isolated candidates further reduces the background from light-quark jets, and a low χ^2 reduces the background from decays of different long-lived particles within the event, owing to the good resolution of the silicon tracking detector in the z direction. We use the same final selection originally devised for the $B_s^0 \rightarrow K^-\pi^+$ search [10], whose simulation has proven to be nearly optimal also for detection of $B_s^0 \rightarrow \pi^+\pi^-$. This includes the following criteria: $I_B > 0.525$, $\chi^2 < 5$, $d > 120 \mu\text{m}$, $d_B < 60 \mu\text{m}$, and

$L_T > 350 \mu\text{m}$.

At most one B candidate per event is found after this selection, and a mass ($m_{\pi^+\pi^-}$) is assigned to each, using a charged pion mass assignment for both decay products. The resulting mass distribution is shown in Fig. 2, and is dominated by the overlapping contributions of the $B^0 \rightarrow K^+\pi^-$, $B^0 \rightarrow \pi^+\pi^-$, and $B_s^0 \rightarrow K^+K^-$ modes [14, 17], with backgrounds coming from mis-reconstructed multi-body b -hadron decays (physics background) and random pairs of charged particles (combinatorial background). A $B^0 \rightarrow K^+K^-$ signal would appear in this distribution as an enhancement around $5.18 \text{ GeV}/c^2$, while a $B_s^0 \rightarrow \pi^+\pi^-$ signal is expected at the nominal B_s^0 mass of $5.3663 \text{ GeV}/c^2$, where other more abundant modes also contribute [10].

We used an extended unbinned likelihood fit, incorporating kinematic (kin) and particle-identification (PID) information, to determine the fraction of each individual mode in the sample. The likelihood is defined as

$$\mathcal{L} = \frac{\nu^N}{N!} e^{-\nu} \cdot \prod_{i=1}^N \mathcal{L}_i \quad (1)$$

where N is the total number of observed candidates, ν is the estimator of N to be determined by the fit, and the likelihood for the i th event is

$$\mathcal{L}_i = (1-b) \sum_j f_j \mathcal{L}_j^{\text{kin}} \mathcal{L}_j^{\text{PID}} + b (f_p \mathcal{L}_p^{\text{kin}} \mathcal{L}_p^{\text{PID}} + (1-f_p) \mathcal{L}_c^{\text{kin}} \mathcal{L}_c^{\text{PID}}), \quad (2)$$

where the index j runs over all signal modes, and the index ‘p’ (‘c’) labels the physics (combinatorial) background terms. The f_j are the signal fractions to be determined by the fit, together with the background fraction parameters b and f_p .

For each charged hadron pair, the kinematic information is summarized by three loosely correlated observables: the squared mass $m_{\pi^+\pi^-}^2$; the charged momentum asymmetry $\beta = (p_+ - p_-)/(p_+ + p_-)$, where p_+ (p_-) is the momentum of the positive(negative) particle; the scalar sum of particle momenta $p_{\text{tot}} = p_+ + p_-$. The above variables allow evaluation of the squared invariant mass m_{a+b-}^2 of a candidate for any mass assignment of the positive and negative decay products (m_{a+}, m_{b-}), using the equation

$$m_{a+b-}^2 = m_{\pi^+\pi^-}^2 - m_{\pi^+}^2 - m_{\pi^-}^2 + m_{a^+}^2 + m_{b^-}^2 - 2\sqrt{p_+^2 + m_{\pi^+}^2} \sqrt{p_-^2 + m_{\pi^-}^2} + 2\sqrt{p_+^2 + m_{a^+}^2} \sqrt{p_-^2 + m_{b^-}^2}, \quad (3)$$

where $p_+ = p_{\text{tot}} \frac{1+\beta}{2}$, $p_- = p_{\text{tot}} \frac{1-\beta}{2}$.

The likelihood terms $\mathcal{L}_j^{\text{kin}}$ describe the kinematic distributions of $m_{\pi^+\pi^-}^2$, β , and p_{tot} variables for the physics signals and are obtained from Monte Carlo simulations. The same distributions for the combinatorial background are instead extracted from real data [18], and are plugged

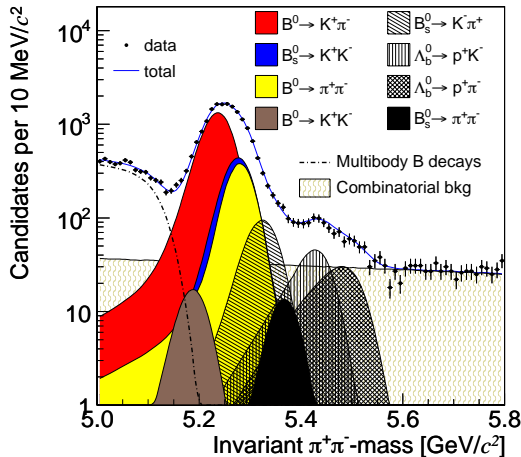


FIG. 2: Mass distribution of reconstructed candidates. The charged pion mass is assigned to both tracks. The sum of the fitted distributions and the individual components of signal and background are overlaid on the data distribution.

TABLE I: Yields and significances of rare mode signals. The first quoted uncertainty is statistical; the second is systematic.

Mode	N_s	Significance
$B^0 \rightarrow K^+ K^-$	$120 \pm 49 \pm 42$	2.0σ
$B_s^0 \rightarrow \pi^+ \pi^-$	$94 \pm 28 \pm 11$	3.7σ

into the likelihood through the $\mathcal{L}_c^{\text{kin}}$ term. In particular, the squared-mass distribution of the combinatorial background is parametrized by an exponential function. The slope is fixed in the fit to the value extracted from an enriched sample of two generic random tracks, containing events passing all requirements of final selections except for vertex quality, replaced by an anti-selection cut $\chi^2 > 40$, which strongly rejects track pairs originating from a common vertex. The likelihood term $\mathcal{L}_p^{\text{kin}}$ describes the kinematic distributions of the background from partially reconstructed decays of generic B hadrons. The $m_{\pi^+\pi^-}^2$ distribution is, in this case, modeled by an ARGUS function [19] convoluted with a Gaussian resolution, while β and p_{tot} distributions are obtained from Monte Carlo simulation.

To ensure the reliability of the search for small signals in the vicinity of larger peaks, the shapes of the mass distributions assigned to each signal have been modeled in detail. Momentum dependence and non-Gaussian resolution tails are accounted for by a full simulation of the detector, while the effects of soft photon radiation in the final state are simulated by PHOTOS [20]. This resolution model was accurately checked against the observed shape of the $3.2 \times 10^6 D^0 \rightarrow K^- \pi^+$ and $140 \times 10^3 D^0 \rightarrow \pi^+ \pi^-$ signals in a sample of $D^{*+} \rightarrow D^0 \pi^+$ decays, collected with a similar trigger selection.

The $D^{*+} \rightarrow D^0 \pi^+$ sample was also used to calibrate

the dE/dx response of the drift chamber to kaons and pions, using the charge of the D^{*+} pion to identify the D^0 decay products. The dE/dx response of protons was determined from a sample of about 167 000 $\Lambda \rightarrow p\pi^-$ decays, where the kinematic properties and the momentum threshold of the trigger allow unambiguous identification of the decay products [21]. PID information is summarized by a single observable κ , defined as:

$$\frac{dE/dx - dE/dx(\pi)}{dE/dx(K) - dE/dx(\pi)} \quad (4)$$

where $dE/dx(\pi)$ and $dE/dx(K)$ are the expected dE/dx depositions for those particle assignments. The average values of κ expected for pions and kaons are by construction 0 and 1. Statistical separation between kaons and pions is about 1.4σ , while the ionization rates of protons and kaons are quite similar in the momentum range of interest. The PID likelihood term, which is similar for physics signals and backgrounds, depends only on κ and on its expectation value $\langle \kappa \rangle$ (given a mass hypothesis) of the decay products. In particular the physics signals model is described by the likelihood term $\mathcal{L}_j^{\text{PID}}$, where the index j univocally defines the particles in the final state, while the background model is described by the two terms $\mathcal{L}_p^{\text{PID}}$ and $\mathcal{L}_c^{\text{PID}}$, respectively for the physics and combinatorial background, that account for all possible pairs that can be formed combining only pions and kaons. In fact muons are indistinguishable from pions with the available dE/dx resolution, and are therefore included within the nominal pion component. For similar reasons, the small proton component in the background has been included within the nominal kaon component. Thus the physics background model allows for independent, charge-averaged contributions of pions and kaons, whose fractions are determined by the fit; while the combinatorial background model, instead, allows for more contributions, since independent fractions of positively and negatively charged pions and kaons are determined by the fit.

From the signal fractions returned by the fit, in agreement with those obtained in the previous iteration of this analysis [10], we calculate the signal yields for the different $B \rightarrow h^+ h'^-$ decay modes. The yields for the $B_s^0 \rightarrow \pi^+ \pi^-$ and $B^0 \rightarrow K^+ K^-$ modes are shown in Table I. The significance is evaluated as the ratio of the yield observed in data to its total uncertainty (statistical and systematic), as determined from a simulation where the size of that signal is set to zero. This evaluation assumes a Gaussian distribution of yield estimates, supported by the results obtained from repeated fits to simulated samples. This procedure yields a more accurate measure of significance than the purely statistical estimate obtained from $\sqrt{-2\Delta\ln(\mathcal{L})}$.

We obtain a 3.7σ significant signal for the $B_s^0 \rightarrow \pi^+ \pi^-$ mode, and we observe an excess at the 2.0σ level for the $B^0 \rightarrow K^+ K^-$ mode. As a check on the method, Figure 3

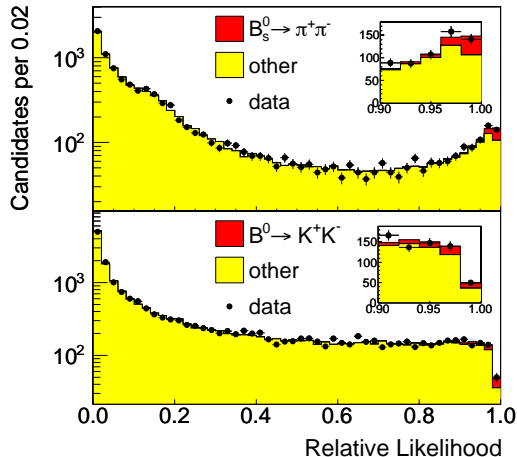


FIG. 3: Distribution of the relative signal likelihood, $\mathcal{L}_S/(\mathcal{L}_S + \mathcal{L}_{\text{other}})$, in the region $5.25 < m_{\pi^+\pi^-} < 5.50 \text{ GeV}/c^2$ for $B_s^0 \rightarrow \pi^+\pi^-$ and $5.10 < m_{\pi^+\pi^-} < 5.35 \text{ GeV}/c^2$ for $B^0 \rightarrow K^+K^-$. For each event, \mathcal{L}_S is the likelihood for the $B_s^0 \rightarrow \pi^+\pi^-$ (top panel) and $B^0 \rightarrow K^+K^-$ (bottom panel) signal hypotheses, and $\mathcal{L}_{\text{other}}$ is the likelihood for everything but the chosen signal, i.e., the weighted combination of all other components according to their measured fractions. Points with error bars show the distributions of data and histograms show the distributions predicted from the measured fractions. Zoom of the region of interest is shown in the inset.

shows relative likelihood distributions for these modes, which are in good agreement with our model.

To avoid large uncertainties associated with production cross sections and absolute reconstruction efficiency, we measure all branching fractions relative to the $B^0 \rightarrow K^+\pi^-$ mode. A frequentist limit [22] at the 90% C.L. is quoted for the $B^0 \rightarrow K^+K^-$ mode. The raw fractions returned by the fit are corrected for the differences in selection efficiencies among different modes, which do not exceed 10%. These corrections are determined from detailed detector simulation, with only two exceptions that are measured from data: the momentum-averaged relative isolation efficiency between B_s^0 and B^0 , and the difference in efficiency for triggering on kaons and pions due to the different specific ionization in the drift chamber. The former is determined as 1.00 ± 0.03 from fully-reconstructed samples of $B_s^0 \rightarrow J/\psi\phi$, and $B^0 \rightarrow J/\psi K^{*0}$ decays [21]. The latter is determined from samples of D^0 mesons decaying into pairs of charged hadrons [18]. We measure the relative branching fractions $\mathcal{B}(D^0 \rightarrow \pi^+\pi^-)/\mathcal{B}(D^0 \rightarrow K^-\pi^+)$ and $\mathcal{B}(D^0 \rightarrow K^+K^-)/\mathcal{B}(D^0 \rightarrow K^-\pi^+)$. The numbers of events are extracted from the available samples of tagged $D^0 \rightarrow \pi^+\pi^-$, $D^0 \rightarrow K^-\pi^+$ and $D^0 \rightarrow K^+K^-$ decays, fitting the invariant $D^*\pi$ mass spectrum [18], while reconstruction efficiencies are determined from the same simulation used for the measurements described in this Letter. Comparison of these

numbers with world measurement averages [23] allows us to extract the correction needed to compensate for the different efficiency of the tracking trigger for kaons and pions. The final corrections applied to our result do not exceed 5% and are independent of particle momentum.

The dominant contribution to the systematic uncertainty on the $B_s^0 \rightarrow \pi^+\pi^-$ branching fraction is due to the dE/dx model, which derives from the statistical uncertainty on the 48 parameters used for the analytical description of the correlated dE/dx response of the two decay products [21]. This uncertainty is evaluated by repeating the likelihood fit 200 times with different sets of those parameters, randomly extracted from a multi-dimensional sphere, centered on the central value of the parametrization, with a radius corresponding to 1σ of statistical uncertainty. The correlations between the parameters are neglected because their total effect, known from Ref. [24], where they have been accounted for in detail, brings a reduction of the final systematic uncertainty because most correlations are negative. The dE/dx -induced systematic uncertainty on each observable is then obtained as the standard deviation of the distribution of that observable, over the ensemble of likelihood fits performed with different sets of parameters. This approach is adequate for our purposes since the statistical uncertainty is greater than or of the same order of the systematic uncertainty.

Further uncertainties are due to the physics background model and the uncertainty on the relative efficiency corrections. The time evolution of the $B_s^0 \rightarrow \pi^+\pi^-$ mode is potentially different from the flavor-specific modes if there is a significant width difference between the mass eigenstates of the B_s^0 , since it contains a superposition of the flavor eigenstates of the B_s^0 meson. This may affect the efficiency of the event selection relative to the normalization mode $B^0 \rightarrow K^+\pi^-$. We derive our result under the assumption that the $B_s^0 \rightarrow \pi^+\pi^-$ mode is dominated by the short-lived B_s^0 component, that $\Gamma_s = \Gamma_d$, and $\Delta\Gamma_s/\Gamma_s = 0.092^{+0.051}_{-0.054}$ [23]. This introduces a small uncertainty which is accounted for in the final quoted systematic uncertainty. A further systematic uncertainty of the order of 10% is included for the $B^0 \rightarrow K^+K^-$ mode to account for a small bias of the fitting procedure observed in simulated samples. Other contributions come from trigger efficiencies, b -hadron masses and lifetimes, and transverse momentum distribution of the Λ_b^0 baryon.

The final results are listed in Table II. Absolute branching fractions are also quoted, by normalizing to world-average values of production fractions and $\mathcal{B}(B^0 \rightarrow K^+\pi^-)$ [23]. The branching fraction measured for the $B_s^0 \rightarrow \pi^+\pi^-$ mode is consistent with and supersedes the previous upper limit ($< 1.2 \times 10^{-6}$ at 90% C.L.), based on a subsample of the current data [10]. It is in agreement with predictions obtained with the pQCD approach [8, 9], but it is higher than most other the-

TABLE II: Measured relative branching fractions of rare modes. Absolute branching fractions were derived by normalizing to the current world-average value $\mathcal{B}(B^0 \rightarrow K^+\pi^-) = (19.4 \pm 0.6) \times 10^{-6}$, and assuming the average values at high energy for the production fractions: $f_s/f_d = 0.282 \pm 0.038$ [23]. The first quoted uncertainty is statistical; the second is systematic.

Mode	Relative \mathcal{B}	Absolute \mathcal{B} (10^{-6})	Limit (10^{-6})
$B^0 \rightarrow K^+K^-$	$\frac{\mathcal{B}(B^0 \rightarrow K^-K^+)}{\mathcal{B}(B^0 \rightarrow K^+\pi^-)} = 0.012 \pm 0.005 \pm 0.005$	$0.23 \pm 0.10 \pm 0.10$	[0.05, 0.46] at 90% C.L.
$B_s^0 \rightarrow \pi^+\pi^-$	$\frac{f_s}{f_d} \frac{\mathcal{B}(B_s^0 \rightarrow \pi^+\pi^-)}{\mathcal{B}(B^0 \rightarrow K^+\pi^-)} = 0.008 \pm 0.002 \pm 0.001$	$0.57 \pm 0.15 \pm 0.10$	–

oretical predictions [5, 6, 25]. The central value for $\mathcal{B}(B^0 \rightarrow K^+K^-)$ is the most precise determination of this quantity to date, and is in agreement with previous experimental results [11, 26] and theoretical predictions [5, 6]. It supersedes the previous CDF limit [10], based on a subsample of the current data.

The present measurements represent a significant step in reducing a source of uncertainty in many theoretical predictions for charmless B -decays. The current result indicates a large annihilation scenario, which is somewhat unexpected for instance in QCDF [27]. This increased precision provides more stringent constraints on the most common phenomenological models, allowing a much more powerful test of the Cabibbo-Kobayashi-Maskawa theory of quark-flavor dynamics and an enhancement of the current sensitivity to the presence of non-standard-model effects.

In summary, we have searched in CDF data for as-yet-unmeasured charmless decay modes of neutral b -mesons into pairs of charged mesons. We report an updated upper limit for the $B^0 \rightarrow K^+K^-$ mode and the first evidence for the $B_s^0 \rightarrow \pi^+\pi^-$ mode and a measurement of its branching fraction.

We thank the Fermilab staff and the technical staffs of the participating institutions for their vital contributions. This work was supported by the U.S. Department of Energy and National Science Foundation; the Italian Istituto Nazionale di Fisica Nucleare; the Ministry of Education, Culture, Sports, Science and Technology of Japan; the Natural Sciences and Engineering Research Council of Canada; the National Science Council of the Republic of China; the Swiss National Science Foundation; the A.P. Sloan Foundation; the Bundesministerium für Bildung und Forschung, Germany; the Korean World Class University Program, the National Research Foundation of Korea; the Science and Technology Facilities Council and the Royal Society, UK; the Russian Foundation for Basic Research; the Ministerio de Ciencia e Innovación, and Programa Consolider-Ingenio 2010, Spain; the Slovak R&D Agency; the Academy of Finland; and the Australian Research Council (ARC).

[1] A. Soni and D. A. Suprun, Phys. Rev. D **75**, 054006 (2007).

- [2] A. J. Buras, R. Fleischer, S. Recksiegel, and F. Schwab, Nucl. Phys. **B697**, 133 (2004).
- [3] D. London and M. Joaquim, Phys. Rev. D **70**, 031502 (2004);
- [4] R. Fleischer, Eur. Phys. J. **C52**, 267 (2007).
- [5] M. Beneke and M. Neubert, Nucl. Phys. **B675**, 333 (2003).
- [6] H.-Y. Cheng and C.-K. Chua, Phys. Rev. D **80**, 114026 (2009); Phys. Rev. D **80**, 114008 (2009).
- [7] C. W. Bauer, S. Fleming and M. Luke, Phys. Rev. D **63**, 014006 (2000).
- [8] A. Ali *et al.*, Phys. Rev. D **76**, 074018 (2007).
- [9] Y. Li, C.-D. Lu, Z.-J. Xiao, and X.-Q. Yu, Phys. Rev. D **70**, 034009 (2004).
- [10] A. Aaltonen *et al.* (CDF Collaboration), Phys. Rev. Lett. **103**, 031801 (2009).
- [11] K. Abe *et al.* (Belle Collaboration), Phys. Rev. Lett. **98**, 181804 (2007).
- [12] Throughout this paper, C-conjugate modes are implied and branching fractions indicate CP-averages.
- [13] D. Acosta *et al.* (CDF Collaboration), Phys. Rev. D **71**, 032001 (2005); A. Sill (CDF Collaboration), Nucl. Instrum. Methods A **447**, 1 (2000); A. Affolder *et al.*, Nucl. Instrum. Methods A **453**, 84 (2000); T. Affolder *et al.*, Nucl. Instrum. Methods A **526**, 249 (2004).
- [14] A. Abulencia *et al.* (CDF Collaboration), Phys. Rev. Lett. **97**, 211802 (2006).
- [15] CDF II uses a cylindrical coordinate system in which ϕ is the azimuthal angle, r is the radius from the nominal beam line, and z points in the proton beam direction, with the origin at the center of the detector. The transverse plane is the plane perpendicular to the z axis.
- [16] Isolation is defined as $I_B = p_T(B)/[p_T(B) + \sum_i p_{T_i}]$, where $p_T(B)$ is the transverse momentum of the B candidate, and the sum runs over all other tracks within a cone of radius 1, in η - ϕ space around the B flight-direction.
- [17] A. Aaltonen *et al.* (CDF Collaboration), Phys. Rev. Lett. **106**, 181802 (2011).
- [18] F. Ruffini, Ph.D. thesis, Università di Siena, Siena, in preparation.
- [19] Defined as $x \cdot \sqrt{1 - (x/x_0)^2} \cdot e^{-c_A \cdot (x/x_0)^2}$ if $x < x_0$, where $x = m_{\pi^+\pi^-}^2$. The cutoff x_0 is extracted from the simulation while the coefficient c_A is a free parameter in our fit. See H. Albrecht *et al.* (ARGUS Collaboration), Phys. Lett. B **241**, 278 (1990).
- [20] E. Barberio and Z. Was, Comput. Phys. Commun. **79**, 291 (1994).
- [21] M.J. Morello, Ph.D. thesis, Scuola Normale Superiore, Pisa, Fermilab Report No. FERMILAB-THESIS-2007-57 (2007).
- [22] G. J. Feldman and R. D. Cousins, Phys. Rev. D **57**, 3873 (1998).
- [23] K. Nakamura *et al.*, J. Phys. G **37**, 075021 (2010).

- [24] A. Aaltonen *et al.* (CDF Collaboration), arXiv:1108.5765 [hep-ex], (2009).
- [25] J.-F. Sun, G.-H. Zhu, and D.-S. Du, Phys. Rev. D **68**, 054003 (2003).
- [26] B. Aubert *et al.* (BABAR Collaboration), Phys. Rev. D **75**, 012008 (2007).
- [27] G. Zhu, arXiv:1106.4709 [hep-ph].